HYDROLOGICAL PROCESSES
Hydrol. Process. **20**, 267–287 (2006)
Published online 26 August 2005 in Wiley InterScience (www.interscience.wiley.com). DOI: 10.1002/hyp.5902

Effect of morphology and discharge on hyporheic exchange flows in two small streams in the Cascade Mountains of Oregon, USA

Steven M. Wondzell*
Olympia Forestry Sciences Laboratory, Pacific Northwest Research Station, USDA Forest Service, Olympia WA 98512, USA

Abstract:

Stream-tracer injections were used to examine the effect of channel morphology and changing stream discharge on hyporheic exchange flows. Direct observations were made from well networks to follow tracer movement through the hyporheic zone. The reach-integrated influence of hyporheic exchange was evaluated using the transient storage model (TSM) OTIS-P. Transient storage modelling results were compared with direct observations to evaluate the reliability of the TSM. Results from the tracer injection in the bedrock reach supported the assumption that most transient storage in headwater mountain streams results from hyporheic exchange. Direct observations from the well networks in colluvial reaches showed that subsurface flow paths tended to parallel the valley axis. Cross-valley gradients were weak except near steps, where vertical and cross-valley hydraulic gradients indicated a strong potential for stream water to downwell into the hyporheic zone. The TSM parameters showed that both size and residence time of transient storage were greater in reaches with a few large log-jam-formed steps than in reaches with more frequent, but smaller steps. Direct observations showed that residence times in the unconstrained stream were longer than in the constrained stream and that little change occurred in the location and extent of the hyporheic zone between low- and high-baseflow discharges in any of the colluvial reaches. The transient storage modelling results did not agree with these observations, suggesting that the TSM was insensitive to long residence-time exchange flows and was very sensitive to changes in discharge. Disagreements between direct observations and the transient storage modelling results highlight fundamental problems with the TSM that confound comparisons between the transient storage modelling results for tracer injections conducted under differing flow conditions. Overall, the results showed that hyporheic exchange was little affected by stream discharge (at least over the range of baseflow discharges examined in this study). The results did show that channel morphology controlled development of the hyporheic zone in these steep mountain stream channels. Copyright © 2005 John Wiley & Sons, Ltd.

KEY WORDS hyporheic zone; stream tracer experiments; transient storage models; groundwater

INTRODUCTION

Numerous studies have shown that hyporheic exchange flows are driven by head gradients created by channel morphologic features at a variety of spatial scales. At the scale of individual bedforms, pressure variations caused by water flowing over bedforms drive flow through the streambed, which is sometimes called pumping exchange (Thibodeaux and Boyle, 1987; Savant *et al.*, 1987; Elliot and Brooks, 1997; Packman and Bencala, 2000). At larger scales, gravity head drives hyporheic exchange flows. At the channel-unit scale, variations in longitudinal gradients associated with pool–riffle or pool–step sequences drive exchange flows vertically through the streambed, as well as laterally through stream banks (Harvey and Bencala, 1993; Morrice *et al.*, 1997; Hill *et al.*, 1998; Storey *et al.*, 2003, Anderson *et al.*, 2005; Gooseff *et al.*, 2005). At the reach scale, head gradients drive exchange flows of stream water through point bars in the meander bends of rivers (Vervier

* Correspondence to: Steven M. Wondzell, US Forest Service, Pacific Northwest Research Station, Olympia Forestry Science Lab, Olympia, WA 98512, USA. E-mail: swondzell@fs.fed.us

Received 23 October 2003
Accepted 7 January 2005

and Naiman, 1992; Vervier *et al*., 1993) between primary and secondary channels (Wondzell and Swanson, 1996, 1999), and between the channel and buried channels, or 'palaeochannels' (Stanford and Ward, 1988), all of which support laterally extensive hyporheic zones. Finally, change in channel constraint at the upper and lower ends of bounded alluvial reaches also drives hyporheic exchange flows (Boulton *et al*., 1998; Baxter and Hauer, 2000).

Stream tracer experiments and transient storage modelling are commonly used to examine hyporheic exchange flows in mountain streams, and these studies have documented a wide range in both the amount of exchange and the size of the transient storage zone. Several of these studies have made comparisons among reaches with widely varying morphology (D'Angelo *et al*., 1993; Edwardson *et al*., 2003; Gooseff *et al*., 2003b; Harvey *et al*., 2003). Some of these have been designed to compare geomorphically distinct reaches, e.g. the comparison of three mountain streams with different parent lithology which showed that attendant differences in saturated hydraulic conductivity strongly influenced hyporheic exchange (Valett *et al*., 1996; Morrice *et al*., 1997). However, the effect of a specific morphologic feature cannot be isolated when a variety of morphologic features co-occur within a single reach. Further, interpretation of these studies has been hampered by difficulties in proportioning transient storage into in-channel and hyporheic components (Harvey *et al*., 1996; Hall *et al*., 2002), and results of interstream comparisons are often confounded by stream size.

Studies using numerical groundwater flow models have begun to identify the specific effects of individual factors on hyporheic exchange flows, including channel morphology (Kasahara and Wondzell, 2003; Gooseff *et al*., 2005), lateral groundwater inflows and changes in discharge (Storey *et al*., 2003), and sediment heterogeneity (Cardenas *et al*., 2004). In general, these studies show that hyporheic exchange occurs from distinct zones of aquifer recharge (downwelling) and discharge (upwelling) that are linked to a nested series of flow paths varying in both path length and residence time. Work by Kasahara and Wondzell (2003) showed that exchange flows resulting from steps accounted for approximately 50% of the hyporheic exchange flow in mountain streams and that residence times of exchange flows around steps were typically shorter than 25 h. Further, sensitivity analyses using groundwater flow models predicted that large steps would drive more hyporheic exchange flow in a stream reach than would many smaller steps, even if a sufficient number of small steps are present to account for an equal amount of elevation loss over the length of the simulated stream reach (Kasahara, 2000).

Hyporheic exchange flows also respond to changes in stream discharge. Several workers have reported that the extent of the hyporheic zone contracts in response to increased groundwater inflows and stream discharge during storms, and it expands as catchments dry and stream discharge decreases (Gilbert *et al*., 1990; Boulton *et al*., 1992, 1998; Vervier *et al*., 1992; White, 1993; Williams, 1993). Results of several stream-tracer experiments comparing streams of different sizes and experiments repeated under different flow conditions support this prediction (D'Angelo *et al*., 1993; Harvey and Bencala, 1993; Morrice *et al*., 1997; Butturini and Sabater, 1999). Other studies are contradictory, however. Tracer tests by Legrand-Marcq and Laudelout (1985) showed that the size of the transient storage zone decreased as stream discharge increased from 0·3 to 2 l s^{-1}, but was constant as discharge increased from 2 to 12 l s^{-1}. However, tracer tests by Hart *et al*. (1999) showed that the size of the transient storage zone was independent of discharge, but exchange flows increased as discharge increased.

Several authors have identified problems with the transient storage models (TSMs) used to analyse stream tracer tests that call these results into question (Harvey *et al*., 1996; Wagner and Harvey, 1997, 2000). Problems include the high sensitivity of TSM parameters to experimental conditions (Harvey and Wagner, 2000), insensitivity to long-time-scale exchange flows (Harvey *et al*., 1996) which are exacerbated through the use of an exponential residence time distribution (Haggerty *et al*., 2002), and inability to represent physical processes correctly at late time (Marion *et al*., 2003; Zaramella *et al*., 2003).

Alternative approaches, using groundwater flow models, have also demonstrated that hyporheic exchange flows are sensitive to changing stream discharge and provide a mechanistic explanation. These studies have shown that increased groundwater inflows from adjacent hillslopes can be sufficient to reverse head gradients along the stream margin, substantially decreasing both the extent of the hyporheic zone and the amount of

hyporheic exchange flow (Harvey and Bencala, 1993; Wroblicky *et al*., 1998; Storey *et al*., 2003). However, decreases in the extent of the hyporheic zone during large storms may have relatively little effect on the amount of exchange flow (Wondzell and Swanson, 1996). Also, flume studies have shown that the pressure gradients that drive pumping exchange increase with stream flow velocity (Savant *et al*., 1987; Thibodeaux and Boyle, 1987; Elliot and Brooks, 1997; Packman and Bencala, 2000).

The objective of this study was to evaluate the influence of channel and valley-floor morphology and stream discharge on the development of hyporheic zones in small mountain streams. Stream tracer experiments were conducted in four geomorphically distinct colluvial reaches located in two mountain streams. The two streams varied in the degree of bedrock constraint. Within the constrained and unconstrained streams, sampling stations separated stream reaches with large steps formed by log jams from reaches where the morphology was controlled by individual logs or boulders that formed a series of small pool–step sequences. To examine the effect of changing discharge, the stream tracer experiments were conducted twice: at low baseflow in late summer, and early the next summer under high baseflow conditions. Movement of tracer through the hyporheic zone was followed with direct observations from well networks, and the reach-integrated influence of hyporheic exchange was evaluated using the transient storage model OTIS. The large number of observation wells located in relatively dense networks near the centre of each stream reach provided independent estimates with which to evaluate both the TSM results and a variety of comparative metrics derived from TSM parameters and commonly used in hyporheic studies. A fifth tracer experiment in a nearby reach scoured to bedrock provided an opportunity to compare the effect of in-channel transient storage with the combined effect of in-channel and hyporheic storage in the colluvial reaches.

METHODS

Study site description

Investigations were conducted in two small, steep-mountain streams, WS1 and WS3 (Figure 1a and b), draining 100 ha catchments, located in the H. J. Andrews Experimental Forest in the western Cascade Mountains of Oregon, USA (44°10′N, 122°15′W). Stream channel and valley-floor morphology in these streams are dominantly shaped by debris flows; but these occur infrequently, with return intervals between 50 and several hundred years. Debris flows scour some reaches to bedrock, but in other reaches deposit a poorly sorted mix of boulders, cobbles, gravels and finer textured sediment called colluvium. The colluvium rarely exceeds 2 m in depth. In forested systems, debris flows also deposit logs and may form log jams. These headwater mountain streams are not competent to move large logs or boulders, even during major floods, so that the gross morphology of the channel and valley floor changes little from year to year. Debris flows have not occurred in the WS1 study reach since the stream gauge was installed in the 1950s. Debris flows occurred in WS3, in the winter of 1964–65 and again in the winter of 1995–96, during 50- to 100-year return-interval storms. The 1964 debris flows scoured the channel of WS3, so that the study reach contained little sediment or large wood before 1996 (Nakamura and Swanson, 1993). Debris flows in 1996 formed two large log jams in the study reach and filled the channel above the log jams with sediment (Figure 1b).

The valley floor of WS1 is relatively unconstrained, averaging 13·7 m wide and is 3·5 times wider than the active channel over the length of the study reach. Bedrock constraint is greater in WS3, so that the valley floor averages only 8·5 m wide, some 2·3 times wider than the active channel. Both channels are steep, with longitudinal gradients averaging 13%. Annual low flows occur at the end of the summer dry season, with discharge less than 1 l s^{-1} in WS1 and 2 to 3 l s^{-1} in WS3. Baseflows during the wet winter season range from 10 to 20 l s^{-1} in both watersheds. The floods of record generated a discharge of nearly 2·4 m^3 s^{-1} in WS1 and an estimated discharge of 1·7 m^3 s^{-1} in WS3 (where debris flows destroyed the stream gauge). Tracer tests were conducted in the late summer of 1997 and were repeated in early summer of 1998. Peak flows reached 710 l s^{-1} in WS1 and 470 l s^{-1} in WS3 during the winter of 1997–98. Major changes in channel

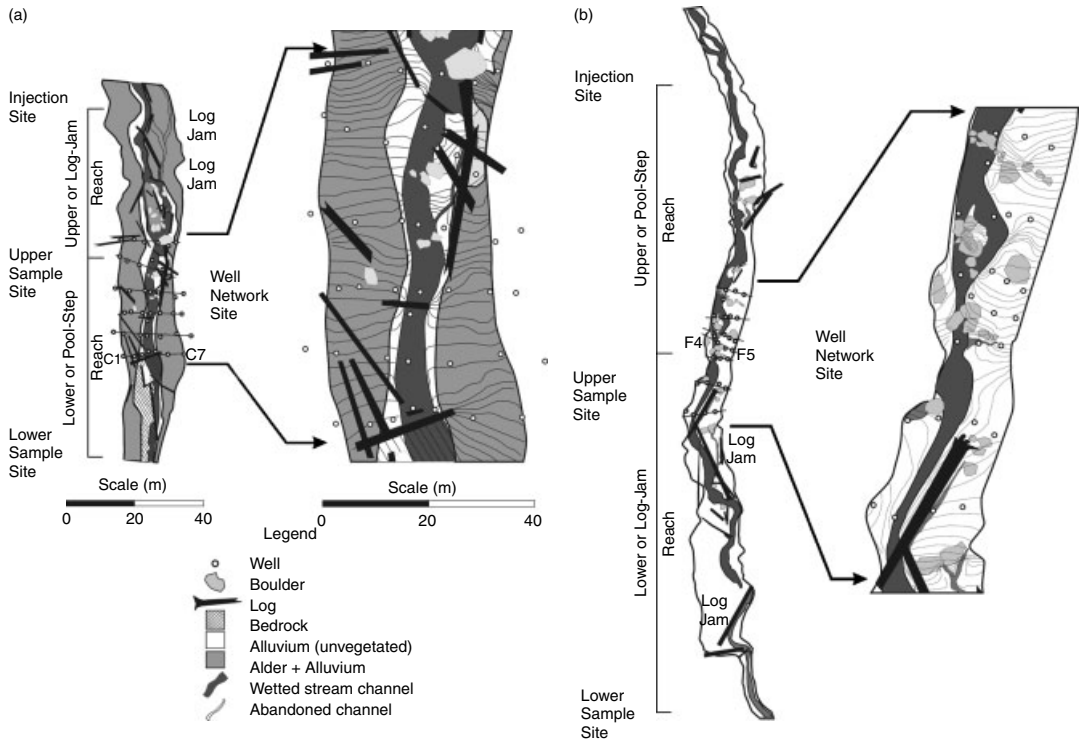

Figure 1. Study reaches in WS1 (a) and WS3 (b) showing location of well networks, boulder and log steps, and log jams on the valley floor of each stream and the injection sites and sample sites used in stream tracer experiments. Cross-sectional profiles of well transects C (WS1) and F (WS3) are shown in Figure 2. Inset maps show close-ups of the well networks in each stream showing water table equipotentials (equipotential intervals: 0·1 m; from Kasahara and Wondzell, (2002))

morphology caused by erosion or deposition of sediment during winter peak flows were not observed. Some minor erosion, however, was observed around two log-formed steps in WS1.

Stream tracer experiments

Stream tracer experiments were designed to compare four geomorphically distinct stream reaches. Two study reaches were delimited in WS1 between upper and lower sampling points (Figure 1a). Two log jams were present in the upper reach, whereas the lower reach was comprised of a series of individual log and boulder steps. Sampling stations in WS3 were located so as to isolate an upper, constrained colluvial reach, characterized by a series of boulder steps, from a lower reach where sediment had collected above two large log jams (Figure 1b). A separate tracer injection experiment was also conducted in a bedrock–gorge reach of WS3, where the stream flows directly on bedrock. Stream tracer experiments were conducted at low baseflow in late summer and early fall of 1997 and again at high baseflow in early summer of 1998. Tracer injection points and sample collection locations were identical at low and high baseflows. The tracer injection in the bedrock–gorge reach of WS3 was not repeated at high baseflow.

A concentrated solution of NaCl was injected at a constant rate until tracer concentrations reached a plateau. Tracer concentrations were measured in the field using electrical conductivity (EC), so that water samples could be collected to characterize breakthrough curves of Cl^--labelled water adequately. Samples were collected in 250 ml HDPE bottles and refrigerated until analysed. Electrical conductivity was measured in the laboratory using a YSI-3200 conductivity meter. A subset of samples from each stream reach, collected during the low baseflow tracer injection, and spanning the observed range in EC, was analysed for Cl^- by ion chromatography (Dionex 4000c). Concentration of Cl^- was highly correlated to EC ($r^2 = 0{\cdot}999$, $n = 21$; $[Cl^-] = 0{\cdot}299EC - 15{\cdot}84$), so EC was used as a surrogate for Cl^- concentration in all analyses.

Direct measurements from wells

Wells and piezometers were established in dense networks near the centre of each experimental reach during the summer of 1997. All wells and piezometers were driven by hand because the study site lacked road access. Large boulders hindered well placement, so that most wells penetrated 1 m, or less, below the ground surface, and the deepest wells penetrated only 1·7 m. Well casings were made from PVC pipe that was 'screened' over the bottom 50 cm by drilling 0·32 cm diameter holes into the bottom of each PVC pipe, at an approximate hole density of 0·25 cm^{-2}. Piezometers were located in the wetted stream channel, and were identical to wells, but were only screened for the bottom 5 cm.

Wells and piezometers were located in closely spaced transects to provide high spatial resolution of subsurface flows (Figure 1a and b). The well network in WS1 spans a 29 m length of stream channel and is comprised of seven piezometers and 30 wells, arranged in six transects spanning the width of the valley floor. Transects typically had six wells, located on the stream bank, halfway between the stream bank and toe slope, and at the toe of the adjoining hills, on both the left and right sides of the valley. A single piezometer was placed in the middle of the wetted channel on each transect. The well network in WS3 spans a 34 m length of channel and is comprised of eight piezometers and 17 wells, arranged in seven transects. Transects in WS3 usually had only three wells and one piezometer, with a well located at the right valley margin, the left stream bank and the left valley margin. Large boulders often pre-empted placement of wells, however, so that well placement was irregular on many transects. Valley-floor cross-sections were surveyed along each well transect in both catchments, and the longitudinal profile of each study reach was also surveyed.

Water table elevations in wells, head in streambed piezometers, and stream water levels along the outside of each piezometer casing were measured immediately before each stream-tracer experiment. Differences in these measurements between low- and high-baseflow discharge were tested for significance using a paired t-test ($\alpha = 0{\cdot}05$). Horizontal hydraulic gradients within the floodplain and vertical hydraulic gradients (VHGs) through the streambed were calculated; VHG (m m^{-1}) $= \Delta h/\Delta l$, where $\Delta h = h_{\text{stream}} - h_{\text{piezometer}}$ and Δl is the distance between the streambed and the top of the piezometer screen (Baxter *et al.*, 2003). Hydraulic gradients are positive where there is a potential for flow toward the channel (or upwelling) and negative where there is a potential for flow away from the channel (or downwelling). Difference in horizontal and vertical hydraulic gradients between low- and high-baseflow discharge were tested for significance using a paired t-test ($\alpha = 0{\cdot}05$).

EC was measured periodically in each well and piezometer during the tracer experiments and used to estimate the connectivity to the stream. Ideally, direct observations in wells are continued until the tracer reaches a plateau in the stream and throughout the hyporheic zone, so that median travel times and the equilibrium proportion of stream water present in each well can be calculated. These calculations, however, cannot be made for wells that fail to reach a plateau over the duration of the experiment. Because many wells in WS1 did not reach a plateau, despite an apparent plateau in stream water, connectivity was calculated relative to the stream EC measured at a specified time t, corrected for background EC ($t = 0$):

$$\text{Relative Connectivity} = \frac{\text{ECwell}_t - \text{ECwell}_{t=0}}{\text{ECstream}_t - \text{ECstream}_{t=0}} \quad (1)$$

Comparisons of relative connectivity between WS1 and WS3 were only possible for the low-baseflow experiment when tracer injections were of similar duration. Calculations were made for a late-time period, 76 h after the start of the injection experiment. The EC was measured in the WS3 wells at this time but had to be interpolated from measurements made between 55 and 80 h after the start of the tracer injection in WS1.

Comparisons of the low- versus high-baseflow relative connectivity within each well network were calculated for fixed times after the start of the tracer injection (69 h in WS1; 10 h in WS3). In WS1, the time was determined by the duration of the high-baseflow injection which reached plateau in 69 h. In WS3, relative connectivity was calculated from data collected 10 h after the start of the injection, which was the last measurement taken from the network before a small storm substantially increased stream discharge and a second storm terminated the tracer injection experiment. Comparative values of EC from the low-baseflow injections were interpolated from measurements made between 55 and 80 h after the start of the tracer injection in WS1 and between 8 and 22 h in WS3. Because of the different time scales, the changes in relative connectivity between high- and low-baseflow discharges can only be compared within a single stream.

Transient storage modelling

Stream tracer data were analysed with OTIS-P (Runkel, 1998). The OTIS model is a finite-difference model solving paired partial differential equations (Equations (2) and (3)) describing one-dimensional transport of a conservative solute in stream channels:

$$\frac{\partial C}{\partial t} = -\frac{Q}{A}\frac{\partial C}{\partial x} + D\frac{\partial^2 C}{\partial x^2} + \frac{q_{\mathrm{Lin}}}{A}(C_{\mathrm{L}} - C) + \alpha(C_{\mathrm{S}} - C) \tag{2}$$

$$\frac{\mathrm{d}C_{\mathrm{S}}}{\mathrm{d}t} = \alpha\frac{A}{A_{\mathrm{S}}}(C - C_{\mathrm{S}}) \tag{3}$$

where C, C_{L} and C_{S} are typically the concentrations of solute in the stream water, groundwater and transient storage zones respectively, but in this case the background-corrected EC (μS) was used in place of concentration. $Q(\mathrm{m^3\ s^{-1}})$ is volumetric stream discharge, $A(\mathrm{m^2})$ is the cross-sectional area of the stream channel, $D(\mathrm{m^2\ s^{-1}})$ is the dispersion coefficient, $q_{\mathrm{Lin}}(\mathrm{m^3\ s^{-1}})$ is the inflow of groundwater, $\alpha(\mathrm{s^{-1}})$ is the exchange flow coefficient, $A_s(\mathrm{m^2})$ is the cross-sectional area of the transient storage zone, t (s) is time, and x (m) is distance. Stream discharge for each reach was estimated using the stream dilution method with background-corrected EC measured at plateau. Lateral groundwater inflows were taken as the difference in discharge between the top and bottom of each reach.

The transport and storage parameters fitting the tracer test data were determined using inverse modelling with OTIS-P, a newer version of OTIS that uses automated parameter estimation techniques and converges toward an optimal solution for the model parameters (Runkel, 1998). The model would not converge to a solution for the WS1 low-baseflow tracer experiment. However, stream discharge varied by ±10% over the course of each day at low baseflow. This resulted in high daily variation in EC, so that OTIS-P simulations fit to the observed data had very high residual sums of squares. To allow OTIS-P to converge to a solution, daily maximum and minimum values of EC were deleted from the observed data for the period of high EC as the tracer test approached plateau. The complete data set was used from the beginning of the tracer injection, through the period of initial tracer breakthrough, and during the steep rise in EC early in the tracer experiment. The final parameter set fit all early-time data well, and was centred between the daily maxima and minima through the plateau period. The model converged to a solution for all other tracer injections.

The automated fitting routine and the statistical package used in OTIS-P attempts to minimize the squared differences between observed data and model simulations (Runkel, 1998). Results include estimates of parameter uncertainty, which are shown here as 95% confidence intervals around each parameter. Additionally, the Damkohler index DaI was calculated to help evaluate the reliability of parameter estimates, as suggested

by Wagner and Harvey (1997):

$$\mathrm{DaI} = \frac{\alpha(1 + A/A_s)L}{u} \tag{4}$$

where L (m) is the reach length and u(m s^{-1}) is the median stream flow velocity.

Several metrics derived from the TSM parameters were used in pairwise reach comparisons to evaluate the influence of channel morphology, channel constraint, and discharge on the hyporheic zone. Metrics chosen for comparison included the relative size of the hyporheic zone A_s/A, the storage zone residence time

$$T_{\mathrm{Sto}} = \frac{A_s}{A\alpha} \tag{5}$$

which gives the average time a water molecule remains in transient storage (Thackston and Schnelle, 1970), the hydraulic retention factor

$$R_h = \frac{A_s}{Q} \tag{6}$$

which gives the average time a water molecule remains in storage relative to the hydraulic turnover length (Morrice *et al*., 1997), and the relatively new metric

$$F_{\mathrm{med}} \cong [1 - \mathrm{e}^{-L(\alpha/u)}]\frac{A_s}{A + A_s} \tag{7}$$

which gives the proportion of the median travel time resulting from transient storage (Runkel, 2002). While each of these metrics emphasizes a slightly different aspect of transient storage, they have in common an attempt to normalize TSM parameters by some measure of flow conditions in the surface channel to facilitate comparisons between reaches (see Runkel (2002) for an in-depth review).

RESULTS

Direct measurements from well networks

Stream and water table elevations. Subsurface flow paths in both WS1 and WS3 tended to parallel the stream channel and sloped steeply down valley, so that down-valley hydraulic gradients averaged 1·4 times steeper than cross-valley gradients throughout each well network, and this relation changed little between low- and high-baseflow discharges. Stream stage was measured along the outside casing of streambed piezometers and changed little from low- to high-baseflow periods in both the WS1 and WS3 study reaches (Figure 2). Stream stage increased by an average of 2·4 cm in WS1 ($n = 7$; $p = 0{\cdot}023$) when discharge increased from 1·22 to 4·67 l s^{-1}. In WS3, stream stage increased an average of 1·7 cm when discharge increased from 3·23 to 11·46 l s^{-1}, but this increase was not significant ($n = 7$; $p = 0{\cdot}428$). Water table elevations in wells and the head in piezometers, averaged over the well network of each stream changed by less than 1·0 cm from low- to high-baseflow, and these changes were not significant (WS1: $p = 0{\cdot}350$; WS3: $p = 0{\cdot}671$). The shape of the water table was complex, however, with water table heights decreasing along the stream, but tending to increase along the valley margins with the change from low- to high-baseflow discharge. In WS1, the head measured in streambed piezometers and the water table measured in stream-bank wells averaged of 3·0 cm lower at high baseflow than at low baseflow ($p = 0{\cdot}024$). Water table elevations tended to increase more in wells along the valley margin (3·0 cm, $p = 0{\cdot}193$) than in wells located in mid-valley floor positions (0·8 cm, $p = 0{\cdot}486$), but these changes were not significant. Observations in WS3 showed similar trends, with head measured in streambed piezometers dropping an averaging of 2·7 cm ($p = 0{\cdot}190$) and water table

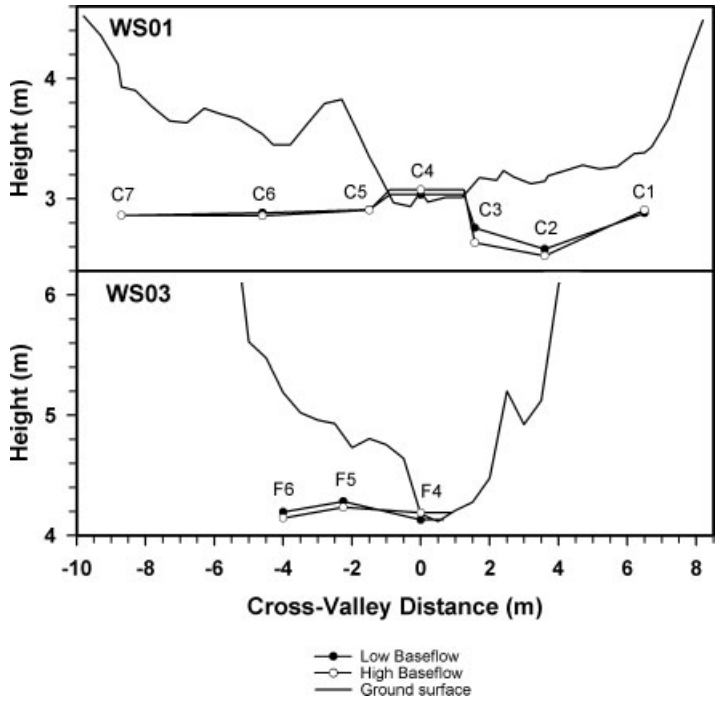

Figure 2. Ground surface, water table elevation and stream stage at low and high baseflows at well transect C (WS1), and well transect F (WS3). Labels C1–C7 and F5–F6 designate wells; labels C4 and F4 designate streambed piezometers

heights in wells along valley margins rising an average of 2·3 cm ($p = 0{\cdot}333$), but changes between low- and high-baseflow discharge were not significant.

Increases in stream stage at high-baseflow discharge combined with decreased head in streambed piezometers (Figures 3 and 4) led to significantly increased VHGs in streambed piezometers, from $-0{\cdot}11$ m m^{-1} at low baseflow in WS1 to $-0{\cdot}22$ m m^{-1} at high baseflow ($p = 0{\cdot}075$), and from $-0{\cdot}35$ m m^{-1} at low baseflow in WS3 to $-0{\cdot}43$ m m^{-1} at high baseflow ($p = 0{\cdot}046$). Very large changes in VHG were observed in streambed piezometers C4 and F4 in WS1 (Figure 3), but this may have been related to local erosion of the streambed around log-formed steps during peak flow events over the winter of 1997–98. With these values deleted, average VHG changed from $-0{\cdot}10$ to $-0{\cdot}14$, and the change was no longer significant ($p = 0{\cdot}201$). Decreased water table heights observed in stream-bank wells, combined with increased stream stage at high baseflow, resulted in horizontal hydraulic gradients through stream banks of WS1 changing significantly, from $-0{\cdot}06$ m m^{-1} at low baseflow to $-0{\cdot}09$ m m^{-1} at high baseflow ($p = 0{\cdot}021$). Horizontal hydraulic gradients from hillslopes to the stream also tended to increase, from 0·03 m m^{-1} at low baseflow to 0·04 m m^{-1} at high-baseflow discharge, but this change was not significant ($p = 0{\cdot}586$). Changes in cross-valley gradients in WS3 were in a similar direction, but of much smaller magnitude, and in no case were changes between low- and high-baseflow discharge significant ($p \geq 0{\cdot}230$).

Hydrologic connectivity. It was not possible to calculate median travel times for many wells in WS1 during the low-baseflow tracer test because those wells did not reach plateau. Consequently, the relative connectivity was calculated from the differences in EC measured in the stream and in each well 76 h after the start of the tracer injection experiment when the stream appeared to have reached plateau. Well and piezometer data from the low-baseflow tracer experiments in both WS1 and WS3 show that nearly all wells located within 4 m of the stream channels reached plateau and that relative connectivity to the

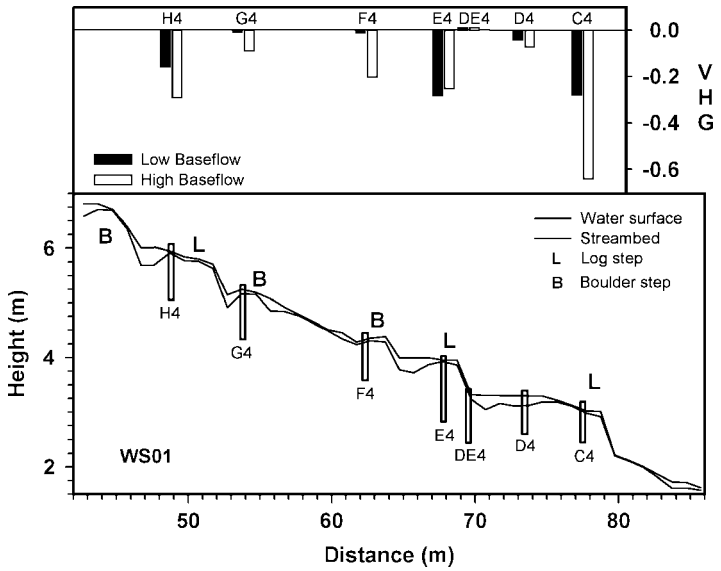

Figure 3. Longitudinal stream profile of WS1 in the region of the well network showing location of piezometers in the stream channel, the streambed surface and the stream water surface at low baseflow discharge (bottom panel) and the VHG through the streambed for each well at low- and high-baseflow discharge (top panel). Labels C4 through H4 designate streambed piezometers

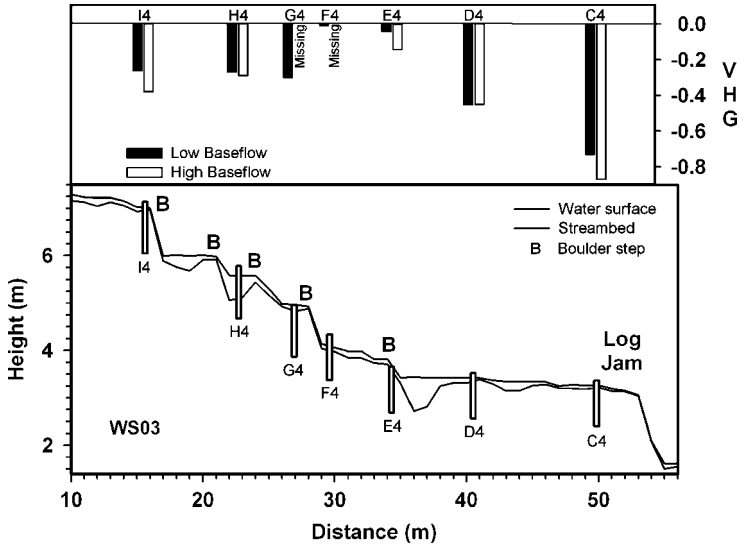

Figure 4. Longitudinal stream profile of WS3 in the region of the well network showing location of piezometers in the stream channel, the streambed surface and the stream water surface at low baseflow discharge (bottom panel) and the vertical hydraulic gradient through the streambed for each well at low- and high-baseflow discharge (top panel). Labels C4–I4 designate streambed piezometers

stream exceeded 0·8 in these wells, whereas less than half the wells in WS1 located more than 4 m from the centre of the stream channel reached plateau (Figure 5). Also, several wells in mid-valley-floor and toe-slope positions appeared to reach plateau even though the relative connectivity was less than 0·2. One piezometer and a few wells located on stream banks, however, also appeared to reach plateau with low relative connectivity.

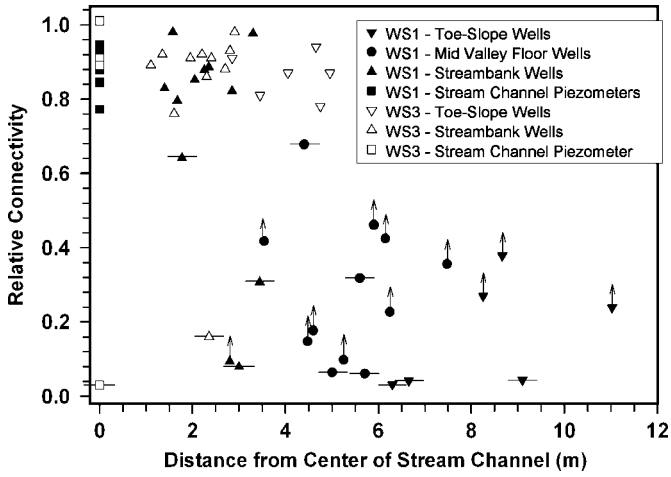

Figure 5. Comparison of relative connectivity between wells and the mainstem channel in WS1 and WS3, 76 h after the start of the low-baseflow tracer experiment in each stream reach. For wells and streambed piezometers with relative connectivity less than 0·7, horizontal lines through symbols denote wells in which EC reached plateau within 76 h and upward-pointing arrows above symbols denote wells in which EC was still increasing after 76 h

Relative connectivity was calculated at a set time after the start of the tracer test (69 h in WS01 and 10 h in WS03) to compare the high- and low-baseflow tracer tests within each well network. Relative connectivity averaged for all 37 wells and piezometers in the WS1 well network was 49%, and did not differ significantly between low- and high-baseflow discharges ($p = 0{\cdot}92$). Similarly, analyses for groups of wells in stream banks, mid-floodplain, and valley-margin locations, and for piezometers located in the centre of the stream channel, were not significantly different between low- and high-baseflow discharges. In most streambed piezometers, increased relative connectivity accompanied increased VHG at high baseflow. In two of seven streambed piezometers, however, relative connectivity decreased by more than 50% at high baseflow discharge even though VHG did not change (DE4) or indicated increased downwelling (H4) (Figure 3).

Relative connectivity averaged for all 24 wells and piezometers in the WS3 well network, 10 h after the start of the injection experiments, was 50% at low baseflow, and decreased to 46% at high baseflow, but this difference was not significant ($p = 0{\cdot}39$). When analysed by location groups, the only significant difference observed in the WS3 well network was for piezometers located in the wetted channel, where relative connectivity decreased from 56% to 34% with the change in discharge from low to high baseflow ($p = 0{\cdot}012$). The VHG measured in these same piezometers, however, increased significantly from $-0{\cdot}35$ m m^{-1} to $-0{\cdot}43$ m m^{-1}, indicating increased potential for downwelling.

Transient storage modelling

Neither the solute injection point nor the sampling locations in each tracer experiment were moved between low- and high-baseflow injections. Keeping the length of the study reaches constant, despite a nearly fourfold increase in stream discharge, resulted in large changes in DaI between low- and high-baseflow tracer injections (Table I). Except for one reach, DaI ranged between 0·2 to 7·0. Experimental conditions for the low-baseflow injection in the upper reach of WS1 resulted in a DaI of 21·1, but coefficients of variation for transport and transient storage parameters were not substantially greater than 0·1 in this reach.

To isolated the effects of pool–step sequences and log jams on transient storage, comparisons were only made between reaches within each watershed under similar flow conditions (Table I, Figure 6). In all cases these comparisons showed that the cross-sectional area of the transient storage zone A_s was significantly

Table I. Summary of tracer injection experimental results from WS1 and WS3. Q, u, and q_{latin} were calculated directly from the tracer injection; A, D, A_s and α were fit to the observed data with inverse modelling using OTIS-P (Runkel, 1998) to minimize the residual sums of squares

Experimental reach	Morphology	Q (l s^{-1})	u (m s^{-1})	q_{latin} (l s^{-1})	TSM parameters				DaI
					A(m^2)	D(m^2 s^{-1})	A_s(m^2)	α(s^{-1} × 10^{-5})	
1997, low flow									
WS1									
Upper (0–49·2 m)	Log jam	1·04	0·0010	0·23	0·39	0·02	1·86	7·40	21·1
Lower (49·2–99·7 m)	Pool–step	1·22	0·0016	0·18	0·23	0·08	0·28	2·18	1·6
WS3									
Upper (0–73·9 m)	Pool–step	2·76	0·0311	−0·02	0·08	0·11	0·48	24·20	4·0
Lower (73·9–183·5 m)	Log jam	3·23	0·0028	0·47	1·30	0·07	1·52	1·34	1·1
WS3 - bedrock (0–137·7 m)	Exposed bedrock	2·49	0·0583	0·13	0·044	0·34	0·007	6·11	0·2
1998, high flow									
WS1									
Upper (0–49·2 m)	Log jam	4·47	0·0207	0·61	0·19	0·20	1·05	15·91	2·4
Lower (49·2–99·7 m)	Pool–step	4·67	0·0167	0·20	0·09	0·01	0·25	62·41	7·0
WS3									
Upper (0–73·9 m)	Pool–step	9·59	0·0801	0·30	0·12	0·16	0·17	18·87	0·4
Lower (73·9–183·5 m)	Log jam	11·46	0·0376	1·87	0·14	0·05	0·70	35·33	6·2

greater in reaches with log jams than in the corresponding reach lacking log jams. These differences were persistent, both between streams and from low- to high-baseflow discharge. Both the storage-zone residence time T_{Sto} and the hydraulic retention factor R_h were greater in reaches with log jams than in the corresponding pool–step reach, and the relative size of the transient storage zone A_s/A was larger in three out of four cases. Neither the exchange coefficient α nor F_{med} showed consistent differences between reaches with and without log jams in these comparisons (Table I, Figure 6).

To isolate the effects of channel constraint, comparisons were only made between reaches with common baseflow discharges and channel morphology. There were no significant differences in A_s between reaches, but there were significant differences in α in three of four between-reach comparisons, but these were inconsistent in direction, with significantly smaller α in the unconstrained reach in two cases, but significantly larger in the other case. Of the comparison metrics, only R_h was consistently greater in unconstrained reaches than in constrained reaches. None of the other metrics showed a consistent pattern of change among the four pairwise comparisons.

To isolate the effects of changing discharge on transient storage, comparisons were only made between tracer experiments conducted at low- and high-baseflow discharge in a given reach (Table I, Figure 7). In three out of four cases, A_s was significantly lower at high baseflow than at low baseflow, and the exchange coefficient α was significantly higher at high baseflow discharge in two cases. Of the comparative metrics, both T_{Sto} and R_h were lower at high baseflow than at low baseflow in all cases, and A_s/A was larger at high baseflow in three of four cases. The F_{med} did not show a consistent pattern of change between streams or between reaches dominated by either pool–step sequences or log jams.

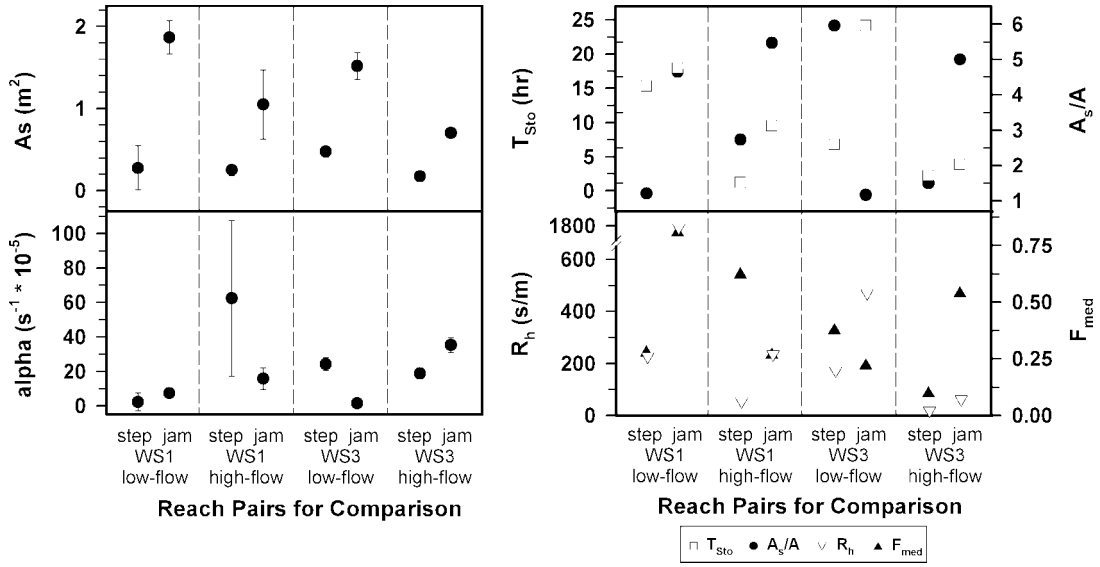

Figure 6. Comparisons of transient storage parameters (A_s, α; 95% confidence intervals) and derived metrics (T_{Sto}, A_s/A, R_h, F_{med}) between corresponding reaches dominated by pool–step sequences (step) or by large log jams (jam). Note that symbols may hide tight confidence intervals. Vertical dashed lines within each panel designate pairs of reaches with similar flow conditions, i.e. comparisons drawn within a single stream at either low- or high-baseflow discharge

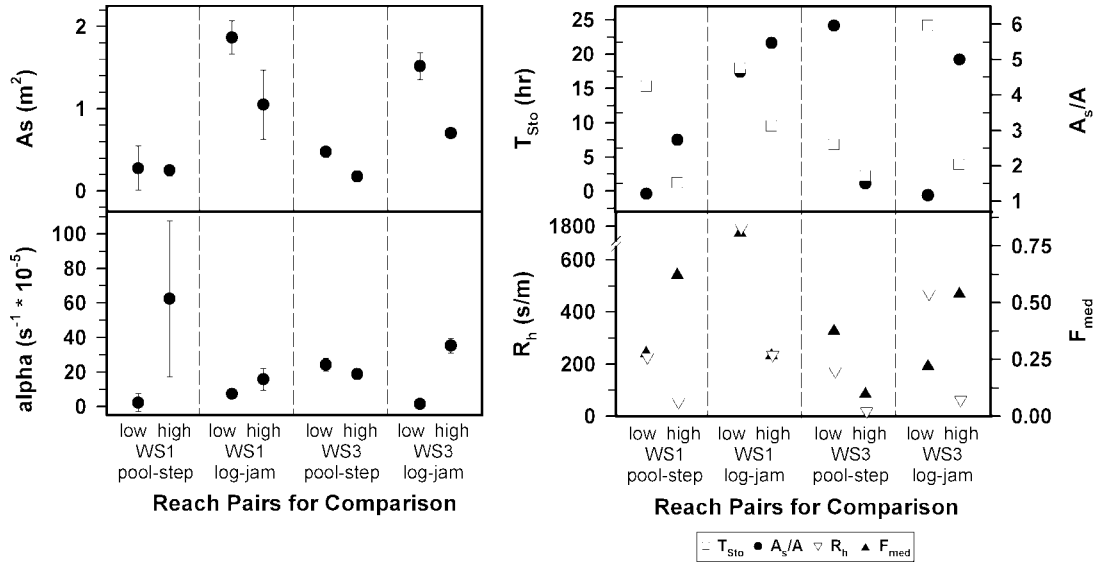

Figure 7. Comparisons of transient storage parameters (A_s, α; 95% confidence intervals) and derived metrics (T_{Sto}, A_s/A, R_h, F_{med}) within a single reach at either low baseflow (low) or high baseflow (high). Note that symbols may hide tight confidence intervals. Vertical dashed lines within each panel designate reaches in which tracer experiments were repeated under different flow conditions

The bedrock reach had the greatest median flow velocity and the smallest values of A_s and T_{Sto} observed in any of the study reaches (Table I). The value of the exchange coefficient α was intermediate between the values observed in the pool–step and log-jam reaches of WS3 during low baseflow, when discharge was similar in all three reaches.

DISCUSSION

Morphologic controls on hyporheic exchange flow

The morphologic features that drive hyporheic exchange flows are controlled by geomorphic processes acting at both reach and catchment scales (Montgomery and Buffington, 1997; Wondzell and Swanson, 1999). At the catchment scale, the balance between sediment supply and sediment-transport capacity controls sediment storage and channel morphology (Montgomery and Buffington, 1997). External forcing factors can alter expected relations. For example, the degree of bedrock constraint determines the width of valley floors, and thereby determines whether space is available for the lateral migration of streams, which leads to construction of point bars and multiple channels (Grant and Swanson, 1995). In steep headwater streams draining forested catchments, large logs may control sediment storage (Nakamura and Swanson, 1993; Montgomery *et al*., 1996). This was the case in both WS1 and WS3, where logs and boulder aggregations frequently obstructed the stream channel, trapping sediment, and forming small steps above individual logs or boulder aggregations. Log jams were infrequent, but formed large steps. Both VHGs measured in streambed piezometers and cross-valley hydraulic gradients between the stream and stream-bank wells indicated a strong potential for stream water to downwell into the sediment trapped above these steps. Further, maps of the water table equipotentials predicted from groundwater flow models showed evidence of short arcuate flow paths around abrupt steps in the longitudinal profile (Figure 1a and b), as described by Harvey and Bencala (1993).

Expected upwelling of hyporheic water below steps was never observed, despite substantial evidence that this should occur. Both the basic description of the physical processes (Harvey and Bencala, 1993) and the hydraulic gradients predicted from groundwater flow models of these study sites suggest that upwelling should be present. Only one streambed piezometer (DE4, Figure 3) had slightly positive VHGs, and that was located immediately below a steep, log-formed step. Positive VHGs have generally not been observed in hyporheic studies at other locations in the Lookout Creek basin, even though groundwater model simulations suggest these should be present (Anderson *et al*., 2005; Gooseff *et al*., 2005). Despite the lack of positive VHGs, neither WS1 nor WS3 are continually losing reaches, because return flows have been observed along their channels. In WS1 water re-emerges into the main channel at the mouth of an abandoned channel in the upper reach and at the contact plane between colluvium stored on the valley floor and exposed bedrock in the lower reach (Figure 1a). In WS3, water re-emerges from several floodplain springs (Figure 1b), where measurements of EC taken during the tracer injection experiments indicate that this water is tracer labelled and is, therefore, a return flow of hyporheic water. Water also seeps from the faces of steep steps, beneath logs and boulders, in both streams, but EC was never measured in these locations. Clearly, these are not continually losing stream reaches, because return flows are present; however, the expected positive VHGs were never observed in piezometers driven into the streambed sediment.

All wells and piezometers in WS3 reached a plateau in less than 76 h, and all but two of these had high relative connectivity (Figure 5). Consequently, calculations of relative connectivity 76 h after the start of the tracer injections provide little basis for comparing wells in different locations within the valley floor. Spatial patterns in relative connectivity were quite different in WS1, where there were clear differences between wells located close to the stream and wells located at greater distances. All streambed piezometers and most near-stream wells reached a plateau at high relative connectivity within 76 h of the start of the tracer experiment, whereas most wells located more than 4 m from the stream had low relative connectivity, and many of these did not reach plateau during the multi-day baseflow tracer injection (Figure 5). Equipotentials from groundwater flow models show that some stream water entering the hyporheic zone would follow long, down-valley-trending flow paths because lateral components of flow are weak over most of the floodplain in WS1 (Figure 1a). Stream water in these flow paths will have very long residence times. Also, some portion of the subsurface flow must be composed of bypass flow, i.e. stream water that was in the hyporheic zone at the tracer injection site and did not get labelled with tracer. Bypass flow cannot be distinguished from lateral groundwater inflows. Both lateral inflows from the adjacent hillslopes and bypass flows mix with tracer-labelled hyporheic water in the floodplain. The long down-valley transport distances combined with lateral

mixing of tracer-labelled water would explain the relatively slow response times of toe-slope and mid-valley wells in WS1.

A few stream-bank wells in both watersheds had slow response times, or reached a plateau with very low relative connectivity to the stream. Preferential flow paths could route long residence-time water throughout the floodplain, and the spacing of the wells might be insufficient to decipher the spatial complexities of such flow paths. Also, stream discharge estimates made from tracer dilution at plateau suggest that there are substantial lateral inflows in most reaches (Table I). This water must be either bypass flow or true groundwater. Because of the structure of the flow net, lateral inflows would be diverted away from downwelling zones above steps and towards areas dominated by return flows. Thus, lateral inflows would be expected to influence some mid-channel and stream-bank wells where head gradients indicate that flows should be towards the stream.

The subsurface flow net in any given reach is complex, responding to the combined effect of the longitudinal gradient of the valley, lateral inflows of groundwater or soil water from adjacent hillslopes, spatial heterogeneity in both the depth and saturated hydraulic conductivity of valley-floor fills, and the effect of channel morphology. The effect of channel morphology on hyporheic exchange flows in mountain streams has been widely studied; but, because all of these factors work in concert, and because of lateral mixing along flow paths, it is impossible to isolate the effects of a single morphologic feature on hyporheic exchange flows using either direct observations from a well field or conservative tracer injection experiments. Studies using numerical groundwater flow models have begun to identify the specific effects of individual factors on hyporheic exchange flows (Kasahara and Wondzell, 2003; Storey *et al*., 2003; Cardenas *et al*., 2004; Gooseff *et al*., 2005). These studies show that hyporheic exchange occurs from distinct zones of aquifer recharge (downwelling) and discharge (upwelling) which are linked to a nested series of flow paths that vary in both path lengths and residence time. Because of the spatial structure of the flow net, indices of hyporheic exchange calculated from well data, such as median residence time or relative connectivity, will not be a simple function of lateral distance from the stream. This nested flow structure would explain the results reported here. Wells located long distances from the stream had long residence times and low relative connectivity. Most stream-bank wells and piezometers located in the streambed appear to be located in aquifer recharge zones at the proximal ends of exchange flow paths and show rapid response with high relative connectivity. A few stream-bank wells and streambed piezometers, however, appear to be located in aquifer discharge zones at the distal ends of exchange flow paths and are dominated by long residence-time exchange flows and low relative connectivity.

Stream discharge and hyporheic exchange flow

Many studies have concluded that changes in stream discharge should result in changed hyporheic exchange flows. There are at least three mechanistic explanations for such a relationship: (1) changes in the pressure field on the streambed resulting from changes in flow velocity and bedform induced turbulence; (2) changing patterns of groundwater inflows; and (3) changes in the effective morphology of the stream channel (e.g. the effect of some morphologic features will be drowned out at high stream stages). The likely role of each of these mechanisms in mountain streams, and their relation to stream discharge, is explored more fully below.

Pressure-head- versus gravity-head-driven exchange flows. The inertial effects of water and pressure variations on the streambed caused by stream flow around and over streambed roughness elements have been studied in laboratory flumes (Elliot and Brooks, 1997; Thibodeaux and Boyle, 1987; Packman *et al*., 2000; Vollmer *et al*., 2002). These studies show that the distance to which stream water penetrates into the streambed and the amounts of exchange flow increase with increasing stream discharge because pressure differences between regions of high and low pressure tend to increase with stream flow velocity. It is difficult to apply these findings directly to mountain streams because the flow conditions in sand- and gravel-bedded flumes are radically different from those in cobble- and boulder-bedded headwater mountain streams. Compare, for example, the flume studies of Elliot and Brooks (1997) with the streams in this study. Surface flow

velocities averaged 17 cm s^{-1} in the flumes, despite an average longitudinal gradient of 0·0011 m m^{-1}. In contrast, the mountain streams in this study had surface flow velocities that averaged 5·5 cm s^{-1} and average longitudinal gradients of 0·12 m m^{-1}. Subsurface flows in these systems are governed by Darcy's law. With a saturated hydraulic conductivity $K = 9{\cdot}2$ m day^{-1}, the experimental conditions in the flumes result in a specific discharge (also known as the Darcian velocity) of 0·01 m day^{-1}. The saturated hydraulic conductivity of the colluvium filling the valley floors of the steep mountain streams averaged 17·9 m day^{-1}, resulting in a specific discharge of 2·2 m day^{-1}. As a result, the ratio between the specific discharge and the surface flow velocity is approximately 1000 times greater in headwater mountain-stream channels than in the experimental channels used in flume studies. The large differences in physical setting should affect the relative importance of pressure-head- and gravity-head-driven hyporheic exchange.

Flume studies have focused on hyporheic exchange at the scale of individual bedforms and have mostly ignored the effects of larger morphologic features. Studies in mountain streams (and other stream systems) have focused at scales ranging from a single riffle to whole reaches, and usually are unable to resolve finer scale effects. Of course, interactions between flow and channel bedforms must drive pumping exchange in steep mountain streams, and this exchange should increase as discharge and flow velocities increase. Unfortunately, the large differences in the physical settings of flume studies versus field studies in mountain streams prevent combining the results of these studies into a comprehensive understanding of the factors driving hyporheic exchange in mountain streams.

Catchment wetness and lateral groundwater inflows. Rates of groundwater discharge in small headwater catchments are related to catchment wetness and, therefore, are positively correlated with stream discharge. Thus, as stream discharge increases, increased groundwater inflows can significantly alter the slope of the water table, forcing exchange flow paths closer to the stream or even eliminate them, as reported by Harvey and Bencala (1993) for St Kevin Gulch, by Wroblicky *et al*. (1998) for Rio Calaveras and Aspen Creek, and by Shibata *et al*. (2004) for the Karuushinai River. The influence of groundwater inflows on lateral hyporheic flow paths must be related to the rate of lateral inflows from adjacent hillslopes and subsurface flow rates through the valley floor. Rates of lateral inflows are controlled by soil moisture content, precipitation (or snowmelt) inputs, and area of the hillslope draining directly to the valley floor. None of these attributes was quantified in this study, nor were they reported in the studies cited above.

Flow through the saturated valley-floor alluvium is governed by Darcy's law (i.e. flow rates are controlled by hydraulic gradient and saturated hydraulic conductivity), which determines the potential, down-valley specific discharge. Many studies have shown that the water table rises and cross-valley gradients increase as the lateral groundwater inflows increase, turning flows more laterally across the floodplain (Wondzell and Swanson, 1996; Shibata *et al*., 2004); this, in turn, increases the cross-sectional area through which flow occurs. Steeper head gradients and larger cross-sectional areas allow increased lateral inputs to be transported to the stream. The degree of change in the subsurface flow net needed to accommodate a given increase in lateral groundwater inputs is dependent on down-valley specific discharge. In general, large changes in the flow net are necessary to accommodate a given increase in lateral inputs where specific discharge is small, whereas small changes in the flow net can accommodate these flows if specific discharge is high.

Lateral groundwater inflows did increase with increasing stream discharge in this study, but the increases were small relative to the specific discharge estimated for saturated valley-floor sediment, so that there was not a significant change in water table elevations at the valley margins. If little or no change in water table morphology accompanies changes in stream discharge, then little or no change in the areal extent of the hyporheic zone or exchange flows of water should be expected. This result stands in sharp contrast to the results of the studies cited above, all of which reported substantial changes in flow nets and hyporheic exchange flows with increasing discharge. The steep longitudinal gradients and coarse colluvial sediment filling the valleys of the mountain streams studied here result in specific discharges ranging between 1·4 and 3·4 m day^{-1}. The lowland Speed River (Storey *et al*., 2003) is very different, with slope $<0{\cdot}006$ m m^{-1} and saturated hydraulic conductivity (K) of streambed sediment averaging 8·6 m day^{-1}, which results in a

specific discharge that is <0·05 m day^{-1}. The low-gradient mountain streams Rio Calaveras and Aspen Creek (Wroblicky *et al*., 1998), with slopes measuring 0·01 and 0·02 m m^{-1} and $K = 0{\cdot}5$ and 0·2 m day^{-1}, resulted in specific discharges of 0·007 and 0·004 m day^{-1}, which were more similar to the lowland Speed River than the steep headwater mountain streams reported in this study, which have specific discharge averaging 2·2 m day^{-1}. Even the moderately steep St Kevin Gulch (Harvey and Bencala, 1993), which has a slope of 0·07 m m^{-1} and $K = 9{\cdot}5$ m day^{-1}, has a specific discharge of 0·6 m day^{-1}, which is much less than in this study. The much lower specific discharge could explain the relatively large influence of lateral groundwater inflows on the extent of the hyporheic zone.

Discharge-caused change in effective channel morphology. Stream discharge could also influence hyporheic exchange flows if changing discharge altered the effective morphology of the stream channel. For example, some pool–step sequences may be submerged at high discharge, changing a stepped-gradient energy profile to a more continuous gradient. Alternatively, secondary channels may become disconnected from surface flow in the primary channel at very low discharge (Edwardson *et al*., 2003). Changes in effective channel morphology associated with changing stream discharge can greatly influence hyporheic exchange. For example, Storey *et al*. (2003) compared changes in hyporheic exchange flows from summer to winter corresponding to a two- to three-fold increase in baseflow discharge. Stream stage did not increase uniformly with increased discharge, so that gravitational head gradients driving exchange flows were reduced by approximately 50% at high baseflow, which decreased hyporheic exchange flows by as much as fivefold. In contrast, doubling lateral groundwater inflows decreased exchange flows by less than 60%. The steep mountain streams studied here contrast markedly with the lower gradient stream studied by Storey *et al*. (2003). In these mountain streams, there was no evidence that the effective channel morphology changed over the fourfold range in baseflow discharges at which stream tracer experiments were conducted.

In summary, the results presented here suggest that spatial patterns, exchange fluxes, and residence-time distributions of hyporheic exchange flows are little affected by stream discharge, at least over the range of baseflow discharges and in the types of mountain stream channel examined in this study. When considered across a wider range of stream types and a wider range of fluctuations in stream discharge, however, the relation between hyporheic exchange flow and both stream size and changes in stream discharge remains unknown. The physical processes that relate changes in stream discharge to hyporheic exchange are likely to vary across a wide range of scales, from individual particles, through the channel-unit scale and up to the reach scale. Further, the relative importance of those processes is also likely to vary in different parts of the valley floor and active stream channel, even within a single stream reach. Identifying the relative importance of different processes and the channel morphologies and flow conditions under which different process are likely to be the dominant drivers of hyporheic exchange flow remains a crucial research question. Developing methodological approaches and designing comparative studies to answer this question remains a substantial challenge.

Transient storage modelling

The 'window of detection' and implications for comparative studies using transient storage modelling. This study used transient storage modelling to compare stream reaches at low- and high-baseflow discharge. The TSM results were in reasonable agreement with many similar studies (D'Angelo *et al*., 1993; Harvey and Bencala, 1993; Morrice *et al*., 1997; Butturini and Sabater, 1999; Hart *et al*., 1999; Edwardson *et al*., 2003), showing significant decreases in A_s and a tendency for increased α with increasing discharge. These results, however, were at odds with direct observations made from the well networks, which showed little change between periods of low- and high-baseflow discharge, despite a nearly fourfold change in discharge.

The conflicting results reported here illustrate a fundamental problem with transient storage modelling that results from the interaction between study reach length and stream flow velocity described by Harvey and Wagner (2000). Flow velocity and reach length, together, determine the time scale of advective transport

through the surface stream channel, which is related to the range of flow path lengths and residence times to which any given stream tracer experiment will be sensitive. Harvey and Wagner (2000) call this the 'window of detection'. In practice, this means that the sensitivity of stream tracer experiments will be biased toward short flow paths and short residence times (Harvey *et al*., 1996; Gooseff *et al*., 2003a). Further, because stream flow velocity increases with discharge, much of the difference between TSM parameters for reaches studied under different flow conditions will result from changes in the dominance of advection relative to transient storage, and not from changes in the physical processes driving hyporheic exchange flow. Unfortunately, there is no way to use transient storage modelling, alone, to determine the spatial extent and residence times of transient storage measured by a given stream tracer experiment.

Direct observations from wells provide an independent measure of both the extent and residence time of hyporheic exchange flow and can be used to confirm comparisons among stream reaches using transient storage modelling. For example, direct observations showed that stream tracer experiments in WS1 were not sensitive to large spatial extent and long residence-time hyporheic exchange flows because EC measured in stream water appeared to reach plateau even though well data showed that many mid-valley and valley-margin wells had not yet reached a plateau (Figure 5). In WS3, however, the stream and most wells reached a plateau during the stream tracer experiment. Thus, comparisons of TSM parameters between WS1 and WS3 cannot determine the effect of channel constraint on hyporheic exchange flows simply because the larger scale exchange flows present in the unconstrained WS1 are invisible given the design of these tracer experiments.

Similarly, the changes in TSM parameters between low- and high-baseflow discharge were most likely an artefact of changing experimental conditions on the 'window of detectability'. Increases in flow velocity with increased discharge decrease the advective time scale of the tracer experiments, so that α excludes more long residence-time exchange flows and A_s excludes the portions of the hyporheic zone through which those flows occur (Harvey *et al*., 1996). The comparative metrics T_{Sto}, A_s/A, and R_h also appear to be substantially influenced by the advective time scale. Even the newer metric F_{med}, which is expressly designed to identify the combined effects of advective travel time and transient storage (Runkel, 2002), produces ambiguous results, with large but inconsistent changes between low- and high-baseflow discharges. Thus, the TSM parameters appear to be too influenced by changing experimental conditions to support between-reach comparisons under changing flow conditions. Further, none of the comparative metrics appears to control sufficiently for changing experimental conditions to support such comparisons.

Uncertainty in estimating TSM parameter values, which is affected both by experimental design and analytical methods, further complicates efforts to compare streams with different discharges, or to make comparisons within a single stream at widely varying discharges (Harvey *et al*., 1996; Wagner and Harvey, 1997). Wagner and Harvey (1997) suggested that the length of the study reach should be adjusted to hold $\mathrm{DaI} \approx 1$. This serves to maintain the relative balance between advective transport and transient storage. However, changing the length of study reaches makes among-reach comparisons difficult, especially in small mountain streams where major changes in channel morphology occur over very short distances. In both WS1 and WS3, for example, sediment stored in 10 to 20 m lengths of channel above log jams dominated hyporheic exchange over 100 to 200 m length study reaches. Obviously, changing the length of a study reach could result in dramatic differences in the morphology of the channel studied. Several studies have also suggested improvements to parameter fitting routines for transient storage modelling to reduce uncertainty associated with visual 'best-fit' solutions (Runkel, 1998; Wagener *et al*., 2002; Scott *et al*., 2003). While constraining experimental design to hold $\mathrm{DaI} \approx 1{\cdot}0$ and improving parameter estimation routines will certainly reduce uncertainty in parameter estimates, they do not solve fundamental problems with the 'window of detectability'.

Because the results of TSM analyses of stream tracer experiments are highly sensitive to experimental design, great caution should be used when comparing stream reaches. Problems with the 'window of detectability' most likely account for the failure of transient storage modelling to characterize the influence of channel constraint and the effects of changing discharge reported in this study. Similar problems were reported by Hall *et al*. (2002), who attempted to relate hyporheic exchange to stream ecosystem processes. Clearly, both the design of tracer experiments and the weaknesses of the analytical model need to be considered when

interpreting the results of any study using a multi-stream comparative approach to examine transient storage and its effects on stream ecosystem processes.

In-channel storage and the effect of channel morphology. Despite the fact that TSM parameters are highly sensitive to experimental design, some comparisons are valid. Comparisons should be restricted to tracer tests performed in different reaches of a single stream under similar flow conditions. In this case, model artefacts should be small relative to the change in the physical factors driving hyporheic exchange flows. In all cases, however, comparisons should be supported with independent observations from well networks or from other approaches. In this study, those criteria restrict the comparisons using TSM parameters to an evaluation of (1) the effect of in-channel processes on transient storage by comparing the bedrock reach of WS3 to the downstream colluvial reaches, and (2) comparisons between reaches in each stream that are dominated by either pool–step morphology or large log jams.

Most studies consider A_s to be a measure of the size of the hyporheic zone, acknowledging that transient storage in the surface channel cannot be separated from the hyporheic zone. Typically, studies assume that the residence time for in-channel transient storage is very short so that its influence is accounted for by the dispersion coefficient rather than the transient storage parameters (Harvey *et al*., 1996). This assumption was tested by conducting a tracer experiment in a bedrock reach of WS3. This reach was scoured free of alluvium, so that stream water flowed over a relatively smooth bedrock surface. Flow velocity was much higher in this reach than in downstream colluvial reaches (Table I). The number and size of pools were similar to those observed in the downstream colluvial reach (Mike Gooseff, personal communication), and zones of shallow water with minimal flow velocity along the stream margins were common. These morphologic features create in-channel transient storage, although the size of the transient storage zone was very small as indicated by A_s. The TSM simulated substantial exchange (α) with the transient storage zone with residence time in storage of 0·71 h. These results show that pools, eddies, and slack water at channel margins do contribute to transient storage in steep headwater streams. Comparisons with low-baseflow parameters from the other reaches in WS3 (Table I), however, show that the in-channel component of transient storage is relatively small and has a relatively short residence time, which lends support for the assumption that most transient storage in headwater mountain streams results from hyporheic exchange processes.

Comparison of TSM parameters among study reaches at either low- or high-baseflow discharge showed that the size of the hyporheic zone and the residence time of water in the hyporheic zone were greater in reaches with large log-jam-formed steps than in reaches with more frequent, but smaller, pool–step sequences (Table I, Figure 6). Most of the comparative metrics also showed large and consistent differences between these reaches, except for F_{med}, which produced ambiguous results, with large but inconsistent changes between the reaches. Log jams in WS3 formed the largest steps observed in this study and significantly widened the otherwise constrained stream channel. Piezometers in the sediment wedge above one of these log jams showed the steepest VHGs and also showed that water downwelled into the accumulated sediment as far as 15 m upstream of the log jam. These results are in agreement with Kasahara (2000), who predicted that a few large steps would have a greater influence on hyporheic exchange flows than would many smaller steps, even if a sufficient number of small steps are present to account for an equal amount of elevation loss over the length of a stream reach.

CONCLUSIONS

This study shows that the morphology of steep mountain-stream channels is a dominant control determining the extent of the hyporheic zone, and both the amount and residence time of stream water flowing through the hyporheic zone. In these streams, subsurface flow paths tended to parallel the valley axis, and lateral head gradients in most places were weak. Immediately above steps, however, both VHGs measured in streambed piezometers and cross-valley hydraulic gradients between the stream and stream-bank wells indicated a strong

potential for stream water to downwell into the sediment trapped above channel-spanning obstructions. Comparison of TSM parameters also showed that the size of the hyporheic zone and the residence time of water in the hyporheic zone were greater in reaches with just a few large steps formed by log jams than in reaches with more frequent, but smaller, pool–step sequences. Direct measurements from the network of piezometers and wells showed that the unconstrained stream had more long residence-time exchange flow paths than did the constrained stream; however, the TSM was insensitive to long residence-time exchange flows, as comparisons of TSM parameters did not show consistent differences with channel constraint.

Observed changes in stream stage and direct measurements of water table elevation and relative connectivity made from well networks showed that little change occurred in the location and extent of the hyporheic zone between low- and high-baseflow discharges. However, significant increases in both VHG through the streambed and cross-valley head gradients through stream banks suggested increased potential for exchange flow at high baseflow discharge. In contrast, the TSM parameter estimates suggested that the size of the transient storage area decreased significantly with increasing discharge, and in only two of four cases were there significant increases in exchange flow. The disagreement between direct observations and TSM parameters at different discharge suggested that TSM results were confounded by changes in the advective time scale of the tracer experiment. The variation in TSM parameters with discharge was most likely an artefact of changing experimental conditions, namely the increased dominance of advection relative to transient storage so that TSM parameters are less sensitive to exchange flows with long residence times. Further, several commonly used comparative metrics that attempt to control for the effects of surface flow condition did not appear to do a better job of distinguishing effects of channel morphology, valley-floor constraint and changing discharge than did the original TSM parameters.

ACKNOWLEDGEMENTS

I thank Ryan Ulrich, Bryan McFadin and especially Tamao Kasahara for help with fieldwork. I thank Stan Gregory and Linda Askenas for their generous support and loan of field equipment. I thank Roy Haggerty, Aaron Packman, Judson Harvey, Peter Huggenberger, Sherri Johnson, Fred Swanson, Tamao Kasahara, Dominique Bachelet and anonymous journal reviewers who provided helpful comments on the manuscript. This work was supported by the National Science Foundation's Hydrologic Sciences Program (EAR-9506669 and EAR-9909564), the H. J. Andrews Long-Term Ecological Research Program (DEB-9632921), and by the USDA Forest Service, Pacific Northwest Research Station's Ecosystem Processes and Aquatic and Land Interactions Programs.

Stream discharge data were provided by the Forest Science Data Bank, a partnership between the Department of Forest Science, Oregon State University, and the US Forest Service Pacific Northwest Research Station, Corvallis, OR. Significant funding for these data was provided by the National Science Foundation Long-Term Ecological Research program (NSF grant numbers BSR-9011663 and DEB-9632921).

The use of trade or firm names in this publication is for reader information and does not imply endorsement by the US Department of Agriculture of any product or service.

REFERENCES

Anderson JK, Wondzell SM, Gooseff MN, Haggerty R. 2005. Patterns in stream longitudinal profiles and implications for hyporheic exchange flow at the H. J. Andrews Experimental Forest, Oregon, USA. *Hydrological Processes* **19**: DOI: 10.1002/hyp.5791.

Baxter CV, Hauer FR. 2000. Geomorphology, hyporheic exchange, and selection of spawning habitat by bull trout (*Salvelinus confluentus*). *Canadian Journal of Fisheries and Aquatic Sciences*. **57**: 1470–1481.

Baxter C, Hauer FR, Woessner WW. 2003. Measuring groundwater–stream water exchange: new techniques for installing minipiezometers and estimating hydraulic conductivity. *Transactions of the American Fisheries Society* **132**: 493–502.

Boulton AJ, Valett HM, Fisher SG. 1992. Spatial distribution and taxonomic composition of the hyporheos of several Sonoran desert streams. *Archiv für Hydrobiologie* **125**: 37–61.

Boulton AJ, Findlay S, Marmonier P, Stanley EH, Valett HM. 1998. The functional significance of the hyporheic zone in streams and rivers. *Annual Review of Ecology and Systematics* **29**: 59–81.
Butturini A, Sabater F. 1999. Importance of transient storage zone for ammonium and phosphate retention in a sandy-bottom Mediterranean stream. *Freshwater Biology* **41**: 593–603.
Cardenas MB, Wilson JL, Zlotnik VA. 2004. Impact of heterogeneity, bed forms, and stream curvature on subchannel hyporheic exchange. *Water Resources Research* **40**: DOI: 10·1029/2004WR003008.
D'Angelo DJ, Webster JR, Gregory SV, Meyer JL. 1993. Transient storage in Appalachian and Cascade mountain streams as related to hydraulic characteristics. *Journal of the North American Benthological Society* **12**: 223–235.
Edwardson KJ, Bowden WB, Dahm C, Morrice J. 2003. The hydraulic characteristics and geochemistry of hyporheic and parafluvial zones in arctic tundra streams, North Slope, Alaska. *Advances in Water Resources* **26**: 907–923.
Elliott AH, Brooks NH. 1997. Transfer of non-sorbing solutes to a streambed with bed forms: laboratory experiments. *Water Resources Research* **33**: 137–151.
Gilbert J, Dole-Olivier M, Marmonier P, Vervier P. 1990. Surface water–groundwater ecotones. In *The Ecology and Management of Aquatic—Terrestrial Ecotones*, Naiman RJ, Decamps H (eds). Man and the Biosphere Series, Vol. 4. UNESCO.
Gooseff MN, McKnight DM, Runkel RL, Vaughn BH. 2003a. Determining long time-scale hyporheic zone flow paths in Antarctic streams. *Hydrological Processes* **17**: 1691–1710.
Gooseff MN, Wondzell SM, Haggerty R, Anderson J. 2003b. Comparing transient storage modeling and residence time distribution (RTD) analysis in geomorphically varied reaches in the Lookout Creek basin, Oregon, USA. *Advances in Water Resources* **26**: 925–937.
Gooseff MN, Anderson JK, Wondzell SM, LaNier J, Haggerty R. 2005. A modelling study of hyporheic exchange pattern and the sequence, size, and spacing of stream bedforms in mountain stream networks. *Hydrological Processes* **19**: DOI: 10.1002/hyp.5790.
Grant GE, Swanson FJ. 1995. Morphology and processes of valley floors in mountain streams, western Cascades, Oregon. In *Natural and Anthropogenic Influences in Fluvial Geomorphology: The Wolman Volume*, Costa JE, Miller AJ, Potter KW, Wilcock PR (eds). Geophysical Monograph Series, Volume 89. AGU: Washington, DC; 83–101.
Haggerty R, Wondzell SM, Johnson MA. 2002. Power-law residence time distribution in the hyporheic zone of a 2nd-order mountain stream. *Geophysical Research Letters* **29**: 13. DOI: 10·1029/2002GL14743.
Hall RO Jr, Bernhardt ES, Likens GE. 2002. Relating nutrient uptake with transient storage in forested mountain streams. *Limnology and Oceanography* **47**: 255–265.
Hart DR, Mulholland PJ, Marzolf ER, DeAngelis DL, Hendricks SP. 1999. Relationships between hydraulic parameters in a small stream under varying flow and seasonal conditions. *Hydrological Processes* **13**: 1497–1510.
Harvey JW, Bencala KE. 1993. The effect of streambed topography on surface–subsurface water exchange in mountain catchments. *Water Resources Research* **29**: 89–98.
Harvey JW, Wagner BJ. 2000. Quantifying hydrologic interactions between streams and their subsurface hyporheic zones. In *Streams and Ground Waters*, Jones JA, Mulholland PJ (eds). Academic Press: San Diego, CA; 3–44.
Harvey JW, Wagner BJ, Bencala KE. 1996. Evaluating the reliability of the stream tracer approach to characterize stream–subsurface water exchange. *Water Resources Research* **32**: 2441–2451.
Harvey JW, Conklin MH, Koelsch RS. 2003. Predicting changes in hydrologic retention in an evolving semi-arid alluvial stream. *Advances in Water Resources* **26**: 939–950.
Hill AR, Labadia CF, Sanmugadas K. 1998. Hyporheic zone hydrology and nitrate dynamics in relation to the streambed topography of a N-rich stream. *Biogeochemistry* **42**: 285–310.
Kasahara T. 2000. *Geomorphic controls on hyporheic exchange flow in mountain streams*. MS thesis, Oregon State University.
Kasahara T, Wondzell SM. 2003. Geomorphic controls on hyporheic exchange flow in mountain streams. *Water Resources Research* **39**(1): 1005. DOI: 10·1029/2002WR001386.
Legrand-Marcq C, Laudelout H. 1985. Longitudinal dispersion in a forest stream. *Journal of Hydrology* **78**: 317–324.
Marion A, Zaramella M, Packman AI. 2003. Parameter estimation of the transient storage model for stream–subsurface exchange. *Journal of Environmental Engineering* **129**: 456–463.
Montgomery DR, Abbe TB, Buffington JM, Peterson NP, Schmidt KM, Stock JD. 1996. Distribution of bedrock and alluvial channels in forested mountain drainage basins. *Nature* **381**: 587–589.
Montgomery DR, Buffington JM. 1997. Channel-reach morphology in mountain drainage basins. *Geological Society of America Bulletin* **109**: 596–611.
Morrice JA, Valett HM, Dahm CN, Campana ME. 1997. Alluvial characteristics, groundwater–surface water exchange and hydrological retention in headwater streams. *Hydrological Processes* **11**: 253–267.
Nakamura F, Swanson FJ. 1993. Effects of coarse woody debris on morphology and sediment storage of a mountain stream system in western Oregon. *Earth Surface Processes and Landforms* **18**: 43–61.
Packman AI, Bencala KE. 2000. Modeling surface–subsurface hydrologic interactions. In *Streams and Ground Waters*, Jones JA, Mulholland PJ (eds). Academic Press: San Diego, CA; 45–80.
Runkel RL. 1998. *One-dimensional transport with inflow and storage (OTIS): a solute transport model for streams and rivers*. USGS Water-Resources Investigations Report 98–4018, Denver, CO.
Runkel RL. 2002. A new metric for determining the importance of transient storage. *Journal of the North American Benthological Society* **21**: 529–543.
Savant SA, Reible DD, Thibodeaux LJ. 1987. Convective transport within stable river sediments. *Water Resources Research* **23**: 1763–1768.
Scott DT, Gooseff MN, Bencala KE, Runkel RL. 2003. Automated calibration of a stream solute transport model: implications for interpretation of biogeochemical parameters. *Journal of the North American Benthological Society* **22**: 492–510.
Shibata H, Sugawara O, Toyoshima H, Wondzell SM, Nakamura F, Kasahara T, Swanson FJ, Sasa K. 2004. Nitrogen dynamics in the hyporheic zone of a forested stream during a small storm, Hokkaido, Japan. *Biogeochemistry* **69**: 83–104.
Stanford JA, Ward JV. 1988. The hyporheic habitat of river ecosystems. *Nature* **335**: 64–66.

Storey RG, Howard KWF, Williams DD. 2003. Factors controlling riffle-scale hyporheic exchange flows and their seasonal changes in a gaining stream: a three-dimensional groundwater flow model. *Water Resources Research* **39**(2): 1034. DOI: 10·1029/2002WR001367.
Thackston EL, Schnelle KB. 1970. Predicting the effects of dead zones on stream mixing. *Journal of the Sanitary Engineering Division, American Society of Civil Engineers* **96**: 319–331.
Thibodeaux LJ, Boyle JO. 1987. Bed-form generated convective transport in bottom sediment. *Nature* **325**: 341–343.
Valett HM, Morrice JA, Dahm CN, Campana ME. 1996. Parent lithology, surface–groundwater exchange, and nitrate retention in headwater streams. *Limnology and Oceanography* **41**: 333–345.
Vervier P, Naiman RJ. 1992. Spatial and temporal fluctuations of dissolved organic carbon in subsurface flow of the Stillaguamish River, (Washington, USA). *Archiv für Hydrobiologie* **123**: 401–412.
Vervier P, Gibert J, Marmonier P, Dole-Olivier J. 1992. A perspective on the permeability of the surface freshwater–groundwater ecotone. *Journal of the North American Benthological Society* **11**: 93–102.
Vervier P, Dobson M, Pinay G. 1993. Role of interaction zones between surface and ground waters in DOC transport and processing: considerations for river restoration. *Freshwater Biology* **29**: 275–284.
Vollmer S, de los Santos Ramos F, Daebel H, Kuhn G. 2002. Micro scale exchange processes between surface and subsurface water. *Journal of Hydrology* **269**: 3–10.
Wagener T, Camacho LA, Wheater HS. 2002. Dynamic indentifiability analysis of the transient storage model for solute transport in rivers. *Journal of Hydroinformatics* **4**: 199–211.
Wagner BJ, Harvey JW. 1997. Experimental design for estimating parameters of rate-limited mass transfer: analysis of stream tracer studies. *Water Resources Research* **33**: 1731–1741.
White DS. 1993. Perspectives on defining and delineating hyporheic zones. *Journal of the North American Benthological Society* **12**: 61–69.
Williams DD. 1993. Nutrient and flow vector dynamics at the hyporheic/groundwater interface and their effects on the interstitial fauna. *Hydrobiologia* **251**: 185–198.
Wondzell SM, Swanson FJ. 1996. Seasonal and storm dynamics of the hyporheic zone of a 4th-order mountain stream. I: hydrologic processes. *Journal of the North American Benthological Society* **15**: 1–19.
Wondzell SM, Swanson FJ. 1999. Floods, channel change and the hyporheic zone. *Water Resources Research* **35**: 355–368.
Wroblicky GJ, Campana ME, Valett HM, Dahm CN. 1998. Seasonal variation in surface–subsurface water exchange and lateral hyporheic area of two stream–aquifer systems. *Water Resources Research* **34**: 317–328.
Zaramella M, Packman AI, Marion A. 2003. Application of the transient storage model to analyze advective hyporheic exchange with deep and shallow sediment beds. *Water Resources Research* **39**(7): 1198. DOI: 10·1029/2002WR001344.

